

# Characterization of monochlorobenzene contamination in soils using geostatistical interpolation and 3D visualization for agrochemical industrial sites in southeast China

Lixia Ren<sup>1</sup>, Hongwei Lu<sup>1,2</sup>, Li He<sup>1,2\*</sup>, Yimei Zhang<sup>3</sup>

<sup>1</sup>North China Electric Power University, China  
School of Renewable Energy

<sup>2</sup>North China Electric Power University, China  
State Key Laboratory of Alternate Electrical Power System with Renewable Energy Sources

<sup>3</sup>North China Electric Power University, China  
Suzhou Research Academy

\*Corresponding author's e-mail: li.he@ncepu.edu.cn

**Keywords:** Soil pollution, monochlorobenzene, POPs, geostatistical interpolation, 3D visualization.

**Abstract:** Persistent organic pollutants (POPs) originating from agrochemical industries have become an urgent environmental problem worldwide. Ordinary kriging, as an optimal geostatistical interpolation technique, has been proved to be sufficiently robust for estimating values with finite sampled data in most of the cases. In this study, ordinary kriging interpolation integrate with 3D visualization methods is applied to characterize the monochlorobenzene contaminated soil for an agrochemical industrial site located in Jiangsu province. Based on 944 soil samples collected by Geoprobe 540MT and monitored by SGS environmental monitoring services, 3D visualization in terms of the spatial distribution of pollutants in potentially contaminated soil, the extent and severity of the pollution levels in different layers, high concentration levels and isolines of monochlorobenzene concentrations in this area are provided. From the obtained results, more information taking into account the spatial heterogeneity of soil area will be helpful for decision makers to develop and implement the soil remediation strategy in the future.

## Introduction

With the increasing demand for organic matters along with industrial development, persistent organic pollutants (POPs) originating from agrochemical industries have become an urgent environmental problem worldwide (Lee et al. 2006, Lisowska 2010, Rosinska and Dabrowska 2011, Ren et al. 2014). The process is often hidden, cumulative and not reversible, which has severely disturbed the natural geochemical cycle of ecosystems through inhalation and/or ingestion (Włodarczyk-Makula 2012, Barchanska et al. 2013). In recent decades, a variety of technologies for remediation of PCB contaminated soils have been developed. Generally, these methods can be divided into the following two categories: 1) *in situ* technologies (e.g. bioremediation, phytoremediation, natural attenuation, capping, microwave-generated steam and oxidization-reduction technology) (Agarwal et al. 2007, Helena et al. 2013), and 2) *ex situ* technologies (e.g. thermal treatment, land farming, dechlorination and solvent extraction) (Sato et al. 2010, Ficko et al. 2011).

Related tools have been widely used in visualizing the characterization of soil pollution and then in developing

remediation strategies. With progress in graphical techniques, 3D visualization has become more and more practical in support of soil and environmental sciences (Yang et al. 2007, Bagiński 2008, Patel et al. 2012). Currently, 3D visualization tools have been applied to spatially exhibit the pollutant concentrations in soils, which could help decision makers understand the spatial variability of pollutant concentrations in soils and the pollution characteristics of soils (e.g. fluctuation characteristics, trend, and distinction in different directions) (Liu et al. 2006, Wu et al. 2013).

Moreover, geostatistical interpolation is useful to smooth curves and surfaces when only sparse spatial data can be available. In the interpolation, multivariate analysis is needed to help evaluate and identify spatial patterns of pollution and its possible sources of pollution, through identifying hotspot areas and visualizing the spatial relationships between environmental data and other land features (Zhang et al. 2008, Henriksson et al. 2013, Kaliraj et al. 2013). For example, Ersoy et al. (2004) used both conventional statistics and geostatistical method to determine the extent and severity of the land pollution levels. Liu et al. (2006) mapped the spatial distribution of heavy metals and conducted risk assessment through geostatistical interpolation.

Based on dataset and 3D visualization platform, GIS mapping can be used for creating elemental spatial distribution maps, 3D images and interpretive hazard maps of pollutants (Bhattacharjee et al. 2014). Considering the available information, geostatistical interpolation techniques have been shown great ability in representing pollutants in soils. However, little effort has been taken to integrated interpolation with visualization techniques to characterize POPs contamination in soils for a real world agrochemical industrial site in China; and few attempts have been performed to present the characterization results in multiple visualized forms to help site investigators gain insight into the soil contamination thoroughly. Therefore, this study uses a 3D visualization tool named EVS-Pro to characterize monochlorobenzene (one of the POPs) contamination in the soil at an agrochemical industrial site in Jiangsu province. Multiple forms of visualization for a given 3D soil domain are presented in results section.

Therefore, this study aims to: 1) characterize the spatial distribution of contaminants in the soil through 3D visualization and spatial interpolation techniques under sparse input information; 2) determine the extent and severity of the pollution levels on land contaminated by past processing activity; 3) analyze the areas of high concentration levels according to the distributions of monochlorobenzene concentrations on each layer; 4) provide decision makers with insight into the monochlorobenzene contamination trend at the local site.

## Methodology

### Geostatistical interpolation

Due to detailed on-site investigation and costly data collection, computer-based methods (e.g. geostatistical interpolation) are often adopted to supplement the sparse data over the entire geological space. The interpolation of spatial data refers to a method of calculating other unknown points or all relevant points within the area through known data points within the relatively smaller regions (Emadi and Baghernejad 2014). Ordinary kriging interpolation, known as the method of space covariance optimal geostatistical interpolation technique, is an appropriate option that is frequently used wherein the sampling data have a good correlation in directional bias and/or space distance. It could explain variations in the surface through spatial correlation, which could be reflected by the direction and/or distance between sampling points.

The application of ordinary kriging in soil studies can date back to the 1980s. During the last two decades, the method has been proved to be more widely used in various subfields of soil science such as soil reclamation, soil classification and soil pollution studies than simple kriging and universal kriging (Burgess and Webster 1980). Compared with simple kriging and universal kriging, ordinary kriging that is an exact interpolation technique shows more advantages in analyzing and describing the spatial variable pattern of soil with finite observation points which are irregularly scattered, resulting in smaller estimation variances and smoother maps.

Weight coefficient  $n$  can be obtained by solving the equations based on the principle of kriging interpolation method and from the assurance of the unbiased estimator and minimum variance estimates. The related equations are provided as follows:

$$Z(x_0) = \sum_{i=1}^n \lambda_i Z(x_i) \quad (1)$$

$$\sum_{i=1}^n \lambda_i C(x_i, x_j) - \mu = C(x_i, x_0) \quad (2)$$

$$\sum_{i=1}^n \lambda_i = 1 \quad (3)$$

where  $Z(x_i)$  is a set of discrete sample data that are defined and attached to  $x_i$  ( $i=1, 2, \dots, n$ ) regions.  $Z(x_0)$  is the interpolation of without-measured point  $x_0$ ;  $\lambda$  is the weight obtained from the semivariogram formed by variogram;  $C(x_i, x_j)$  is the covariance between regional sample points;  $C(x_i, x_0)$  is the covariance between regional sample points and interpolation points; and  $\mu$  is the Lagrange multiplier.

### Finite difference gridding

Finite difference gridding (FDG) is used in the 3D visualization environment where the standard gridding methods are inefficient or inapplicable. It has the following functions: 1) grids can be designed by users visually with variable spacing; 2) the geologic layer elevations can be kriging-interpolated directly to the finite difference grid element; and 3) grids can be adaptive and the surrounding gridding can be refined automatically in order to ensure the accuracy of the interpolated results and isosurfaces; 4) adaptive gridding can provide reasonably accurate results that cannot be approximated by any other method (van Es et al. 2014, Fazio and Jannelli 2014).

FDG offers a straight-sided grid domain consisted of variable-sized rectangles. A grid can be defined by the convex hull of geology file and geologic layers in the  $x$ - $y$  plane and  $z$  spacing, respectively. The visualization tool can provide a full spectrum of 3D FDG option with variable spacing in  $x$ ,  $y$  directions and  $z$  spacing that can be set up in FDG subpanels, which can restrict the model domain to be within the FDG range. By extending the range, different layers of the plume, as well as all of the borings and sample locations, can be exploded to match the separated layers.

### Migration model

Soil is widely distributed, and it has an intricate natural degradation system, thus making it difficult to research the process of migration and transformation of its pollutants. Factors such as soil texture, structure, intensity, temperature, course of water supply, types of contaminants, and chemical and physical process of pollutants will have a significant impact on the migration and transformation behavior of environmental pollutants in the soil. Because of the existence of underground water, the large amount of organic and inorganic colloid, plants, animals, and microorganisms, pollutants in the soil are constantly diffused, migrated, transformed, dispersed, adsorbed, decomposed, degraded and accumulated by chemical, physical, and biological reactions (Bezák-Mazur et al. 2007).

It is therefore essential to understand these processes for predicting the variation of pollutant concentration and ultimate destination of pollutants in the soil. Considering the migration and attenuation of pollutants in the soil and according to

the principle of mass conservation, a convection-diffusion mathematical modeling of pollutants migration in saturated and unsaturated soils can be formulated as follows:

$$R_d \frac{\partial c}{\partial t} = \frac{\partial}{\partial x} \left( D_{xx} \frac{\partial c}{\partial x} \right) + \frac{\partial}{\partial y} \left( D_{yy} \frac{\partial c}{\partial y} \right) + \frac{\partial}{\partial z} \left( D_{zz} \frac{\partial c}{\partial z} \right) - \frac{\partial(v_x c)}{\partial x} - \frac{\partial(v_y c)}{\partial y} - \frac{\partial(v_z c)}{\partial z} + \left( \frac{\partial \theta}{\partial t} - \lambda \theta R_d \right) \cdot c \pm M \quad (4)$$

Initial condition:

$$c|_{t=0} = c_0(x, z) \quad (5)$$

Boundary condition:

$$-D \frac{\partial c}{\partial n} \Big|_{\Gamma} = f(x, y, z, t) \quad (6)$$

where  $R_d$  is the retention factor;  $c$  is the pollutant concentration;  $D_{xx}$ ,  $D_{yy}$ , and  $D_{zz}$  are the diffusion coefficients in  $x$ ,  $y$ , and  $z$  directions, respectively;  $v_x$ ,  $v_y$ , and  $v_z$  are the actual average velocity of  $x$ ,  $y$ , and  $z$  directions, respectively;  $\theta$  is the soil moisture content;  $\lambda$  is the attenuation coefficient of pollutants;  $M$  is the source sink term;  $c_0$  is the initial condition;  $f$  is the boundary condition of convection diffusion flux; and  $\Gamma$  is the Neumann boundary condition.

### Simulation framework

The main analytical content of EVS-Pro includes analysis of contaminated soil and groundwater, lakes, rivers, oceans, air and/or noise pollution levels, and so on. Its features include borehole and sample posting and generation of plumes, ore-bodies, cuts, slices, cross sections, and isolines. The embedded 3D fence diagrams have functions of spatial gridding, and geostatistical inference and data analysis. Fig. 1 illustrates a flowchart of the integrated methods, wherein the three-

dimensional structure of soil contamination in different geologic layers (depths) is visualized intuitively. The outputs can eventually support the subsequent tasks like risk assessment and soil remediation design.

## Results

### Materials and methods

An agrochemical industrial site, located in Jiangsu province was investigated in this study. The investigation aimed to gain insight into the POPs pollution in the local soil, based on which risk assessment could be conducted and an appropriate soil remediation strategy could be suggested. To protect the local soil environment quality and the health of local residents potentially exposed to such an environment, the agrochemical plant has been forced to halt its production and the equipment for pesticides production has been dismantled. The results of site investigation showed that 60% of the soil in this area has been contaminated with chlorobenzene, methamidophos, thiophosphoryl chloride, glyphosate and other organic pollutants. Monochlorobenzene has been detected to be the most serious POP with a high-level concentration. In recent years, contaminated land areas have been expanded after the soils soaked with rain, which caused residual chemicals to not only contaminate shallow soils but also have an impact on deep soils or groundwater.

Detailed information with respect to the physicochemical property of sampling sites is shown in Table 1. Soil samples were collected by Geoprobe 540MT which is a direct push type soil sampling tool due to its ability to quickly and efficiently recover soil samples. Sampling at depths was greater than 18 m. The soil-related and stratigraphic parameters and part of soil monitoring data were obtained from environmental monitoring services (i.e. SGS company) through 944 soil samplings. The drilling content of specific detection included coordinates, elevation/depth, boring ID, chemical content, bottom elevation, etc. Data with respect to monochlorobenzene concentrations in the soil over the domain were obtained through site investigation and geostatistical interpolation.

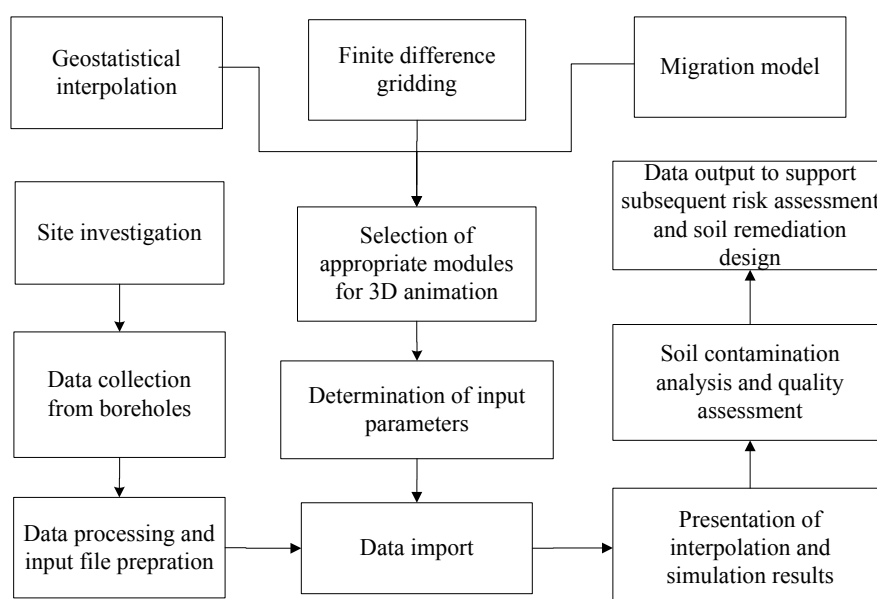


Fig. 1. Flowchart of the characterization approach

**Table 1.** Part of soil parameters of the site

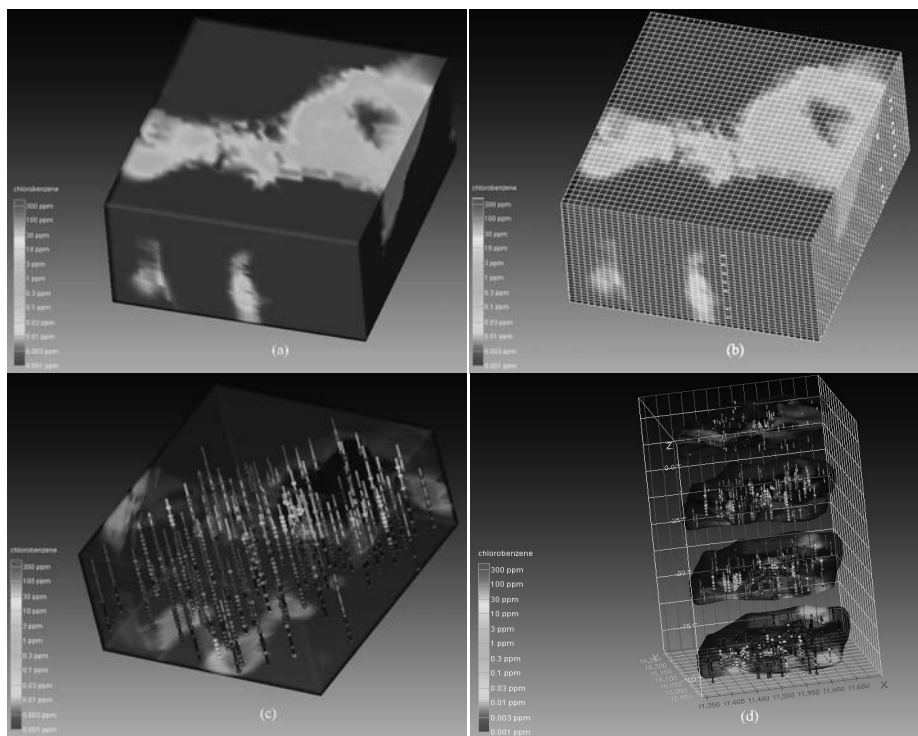
Parameter	Value	Unit
Total soil volume	$6.373 \times 10^4$	$m^3$
Total soil mass	$1.179 \times 10^8$	kg
Chemical volume	0.486	$m^3$
Chemical mass	486.300	kg
Average monochlorobenzene concentration	4.124	mg/kg
Number of samples	944	–

**Result analysis**

The distributions of monochlorobenzene concentration can be exhibited in the Viewer window of the EVS-Pro (Fig. 2(a)). Different sizes and angles of rendering object can be manipulated through setting various values of elevation, scale factor, azimuth, and other relevant parameters. Fig. 2(b) provides the overall concentration in the soil with grids showing on. It is shown that the pollution region mainly occurs in the surface of the soil, and monochlorobenzene concentration is comparatively large in the mid-east region of the soil, where the peak level reaches 3680 mg/kg. Fig. 2(c) presents 944 boreholes of contaminant in the investigated soil domain, whose depth is as much as 16 m. The largest number of sampling points that have identical *X* and *Y* coordinates is 16, and the least is 1. The number of sampling points was determined based on the usage and purpose of workshop in the investigated site. The concentrations of monochlorobenzene in

each geologic layer (which will be detailed in the subsequent paragraph) are computed and exhibited in Fig. 2(d). As shown in the figure, the boreholes and samples have been exploded by the geologic layer.

In the results visualization, four layers (i.e. layers 1 to 4) were divided vertically in terms of soil characteristics, representative of fill-, clay-, sand- and gravel-soil types, respectively. The four layers were determined to be 0 to 2, 2 to 6, 6 to 11, and 11 to 16 meters in depth, respectively. As shown in Fig. 3, the monochlorobenzene concentrations vary with soil depth, and monochlorobenzene migrates from the mid-east to the south direction with increasing soil depth. The distribution of contaminant concentrations and boreholes location on the fill soil layer are also shown in Fig. 3(a). The concentrations at point IDs 104, 105 and 106 in the depth of up to 2 m are higher than other point IDs; this is because they are located around the three pollution sources: raw material storage, production department, and end-product warehouse. This may be due to the properties of production activities in the field and the leakage of pollutants into the environment during production, shipment, and delivery. Compared with layer 1, the contaminant concentrations in the east of layer 2 decrease significantly, yet increase on the southern part appear because of the influence of volatilization, diffusion, adsorption, and migration (Fig. 3(b)). Overall, the ratios of chlorobenzene-contaminated area to the study area keep decreasing, and the location with high-level concentrations is scattered relatively. As shown in Fig. 3(c), the concentrations of chlorobenzene at boreholes 79 and 82 are larger than other ones, indicating that the pollution occurring in layer 3 is consistent with layer 2. Fig. 3(d) provides the



(a) Overall concentrations distribution in soil  
 (b) Overall concentrations distribution in soil with grid  
 (c) Boreholes distribution in soil  
 (d) Concentrations distribution in each geologic layer

**Fig. 2.** Simulated monochlorobenzene concentrations over geologic layers



concentration distributions of monochlorobenzene in layer 4. The highest concentration sampled from the boreholes ID is 79. Compared with the other layers, the monochlorobenzene concentrations in the whole region at layer 4 is reduced except at the southeast region; the pollution is thus more serious than in layer 1, thus enhancing the difficulty in remediating the monochlorobenzene-contaminated soil in this area.

Standard of Soil Quality Assessment for Exhibition Sites 2007 (HJ 350-2007) was selected to assist in identifying contamination areas under different evaluation criteria. Standards A (6 mg/kg) and B (680 mg/kg) were considered in the identification. The soil that complies with standard A can be utilized for various purposes like land use and standard B indicates that the soil should be remediated. Once the chlorobenzene concentrations exceed standard B, soil remediation should not be enforced to put into practice until standard A is satisfied. Figs. 4(a) and 4(b) show the contaminated zone where the chlorobenzene concentrations violate standards A and B, respectively. It is indicated that a large portion of soils does not comply with standard A, whereas a relatively little portion does

not satisfy standard B. Figs. 5 and 6 present the contaminated zones in the four layers, where monochlorobenzene concentrations exceed standards A and B, respectively. It is shown from Fig. 5(a) that the monochlorobenzene complies with standard A in most of the superficial region, yet the central and southwest ones do not. Layer 1, compared with the surface area, do not comply with standard A. In layer 2, the pollution becomes serious, and chlorobenzene is migrating from the middle to the southern part (Fig. 5(b)). In layer 3, the concentrations of chlorobenzene in the southern area increase remarkably, yet the pollution in the middle compartment is alleviated to a certain degree (Fig. 5(a) to 5(c)). In Fig. 5(d), the concentrations of monochlorobenzene violating standard A in layer 4 increase sharply, and the pollution is extremely serious particularly in the southern region. Fig. 6 suggests that the areas without observance of standard B are smaller in layers 1 to 3 than layer 4. This indicates that chlorobenzene pollution becomes alleviated due to natural attenuation. Thus, appropriate soil remediation technologies are suggested for remedial of polluted soils mainly in the upper three layers.

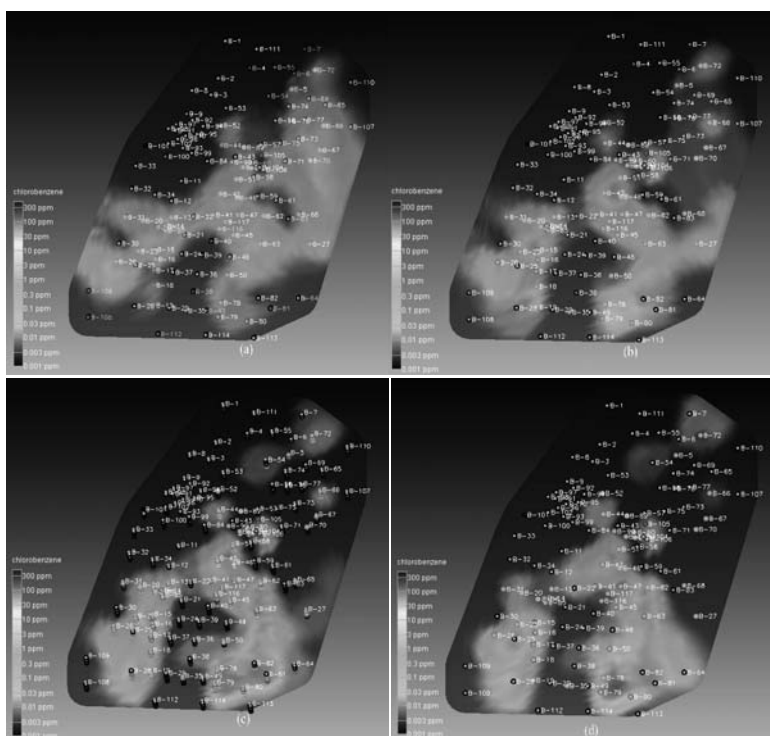


Fig. 3. Distributions of monochlorobenzene concentrations on (a) fill-soil layer, (b) clay layer, (c) sand layer and (d) gravel layer

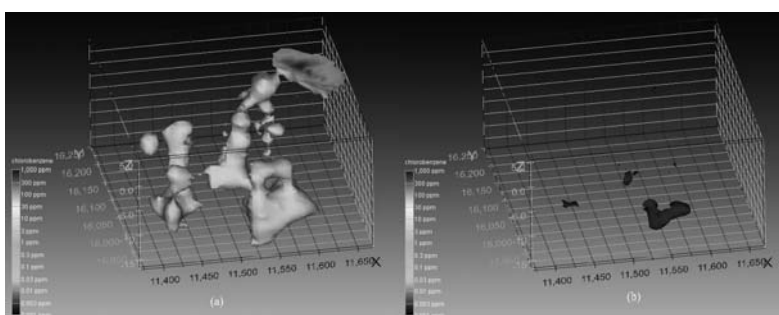
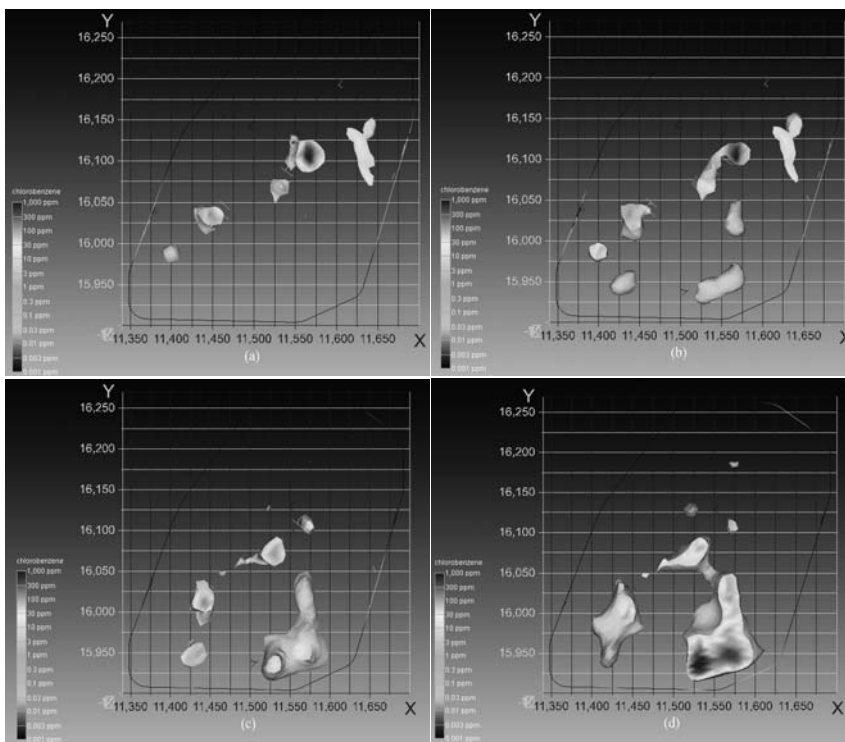
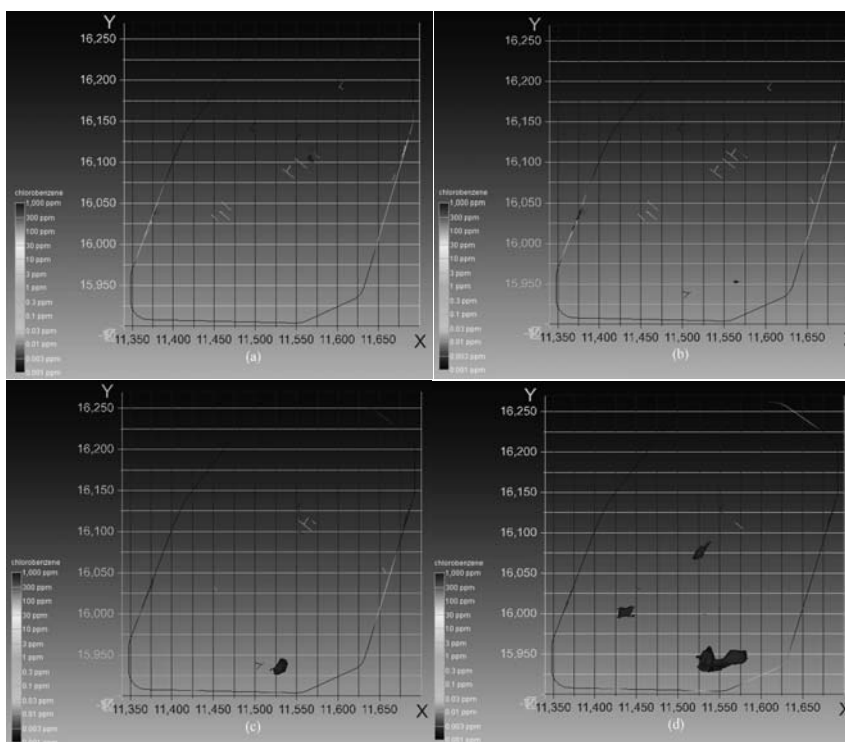


Fig. 4. Distributions of monochlorobenzene concentrations under standards A (a) and B (b) for soil quality assessment



**Fig. 5.** Distributions of monochlorobenzene concentrations under standard A for soil quality on fill-soil layer (a), clay layer (b), sand layer (c) and gravel layer (d) assessment in each layer



**Fig. 6.** Distributions of monochlorobenzene concentrations under standard B for soil quality on (a) fill-soil layer, (b) clay layer, (c) sand layer and (d) gravel layer

The chlorobenzne concentrations can also be presented by isolines through the isolines module. Fig. 7 demonstrates the isolines of monochlorobenzene concentrations in the soil. Several preference settings are shown as follows: the lowest isoline level of contaminant concentrations is 0.001 mg/kg, the

highest is 1.000 mg/kg, the label spacing is 0.4 mg/kg, and the surface offset is 0. These created concentration isolines reflect the undulation shape and spatial-temporal distribution characteristics of chlorobenzne in each layer.

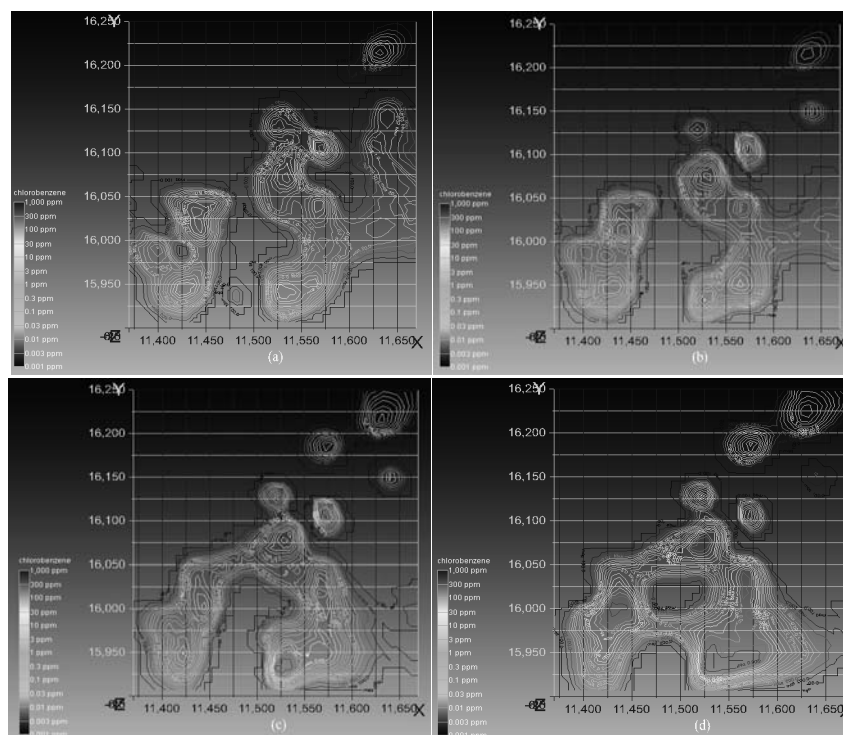


**Fig. 7.** Isolines of monochlorobenzene concentrations on (a) fill-soil layer, (b) clay layer, (c) sand layer and (d) gravel layer

## Discussion and conclusions

This study uses ordinary kriging interpolation and 3D visualization methods to characterize the monochlorobenzene contamination in soils for an agrochemical industrial site in Jiangsu province. The characterization approach integrates kriging interpolation, finite difference gridding, and migration modeling. Kriging is a linear-space valuation method which can consider the spatial structure characteristics of the sample point. FDG ensures the accuracy of the interpolated data and isosurfaces through adapting and refining the surrounding gridding automatically. Through migration modeling, spatial distributions of POPs concentrations in the soil can be simulated.

This paper mainly presents a set of characterization results, including: 1) distributions of monochlorobenzene concentrations on each layer, 2) distributions of contaminant concentrations under A and B for soil quality assessment in overall and each layer; 3) isolines of monochlorobenzene concentrations in each layer; and 4) slice distributions of monochlorobenzene concentrations visualized from different directions. The results indicate that 1) the pollution range mainly appears in the surface of the soil, and monochlorobenzene concentration is comparatively large in the mid-east region of the soil, where the peak level reaches 3680 mg/kg; 2) monochlorobenzene concentrations in the soil vary with soil depth, and monochlorobenzene is migrating from the mid-east to the south with increasing soil depth; 3) the concentrations at four points in the depth of up to 2 m are higher than those at other points; 4) in terms of Standard of Soil Quality Assessment for Exhibition Sites 2007 (HJ 350-2007), a large portion of the contaminated soil does not comply with standard A (6 mg/kg) whereas merely a little portion does not satisfy standard B (680 mg/kg).

These results provide implications for gaining insight into the soil contamination of the site, performing risk assessment of exposing to the site, and providing data support to the development of soil remediation strategies. However, future studies are still desired. For example, sensitivity analysis needs to be performed for understanding the effects of hydrogeological and soil parameters on POPs concentrations in the soil for the agrochemical site; uncertainty analysis is also desired for mitigating such effects. Moreover, the accuracy of the geostatistical interpolation technique could be improved for accommodating increased complexity where extremely sparse data can be available; this would be helpful for compromising the cost paid for data acquisition (through site investigations and geostatistical interpolation) and the accuracy of characterization results.

## Acknowledgements

The authors thank the editor and the anonymous reviewers for their helpful comments and suggestions. This research was supported by the China National Funds for Excellent Young Scientists (51422903), National Natural Science Foundation of China (41271540), Program for New Century Excellent Talents in University of China (NCET-13-0791), and Fundamental Research Funds for the Central Universities.

## References

- Agarwal, S., Al-Abed, S.R. & Dionysiou, D.D. (2007). In situ technologies for reclamation of PCB-contaminated sediments: current challenges and research thrust areas, *Journal of Environmental Engineering*, 133, 12, pp. 1075–1078.
- Bagieński, Z. (2008). Analysis of diffusion within cavity region of pollutants from short-point sources-wind tunnel experimental

- investigation, *Environment Protection Engineering*, 34, 4, pp. 43–50.
- Barchanska, H., Czaplicka, M. & Giemza, A. (2013). Simultaneous determination of selected insecticides and atrazine in soil by Mae-GC-EC, *Archives of Environmental Protection*, 39, 1, pp. 27–40.
- Bezak-Mazur, E., Dabek, L. & Ozimina, E. (2007). Assessing the migration of organic halogen compounds from sewage sludge to a liquid phase, *Environment Protection Engineering*, 33, 2, pp. 5–51.
- Bhattacharjee, S., Mitra, P. & Ghosh, S.K. (2014). Spatial interpolation to predict missing attributes in GIS using semantic Kriging, *Ieee Transactions on Geoscience and Remote Sensing*, 52, 8, pp. 4771–4780.
- Burgess, T.M. & Webster, R. (1980). Optimal interpolation and arithmetic mapping of soil properties: the semivariogram and punctual Kriging, *Soil Science*, 31, pp. 315–331.
- Emadi, M. & Baghernejad, M. (2014). Comparison of spatial interpolation techniques for mapping soil pH and salinity in agricultural coastal areas, northern Iran, *Archives of Agronomy and Soil Science*, 60, 9, pp. 1315–1327.
- Ersoy, A., Yunsel, T.Y. & Cetin, M. (2004). Characterization of land contaminated by past heavy metal mining using geostatistical methods, *Archives of Environmental Contamination and Toxicology*, 46, 2, pp. 162–175.
- Fazio, R. & Jannelli, A. (2014). Finite difference schemes on quasi-uniform grids for BVPs on infinite intervals, *Journal of Computational and Applied Mathematics*, 269, pp. 14–23.
- Ficko, S., Rutter, A. & Zeeb, B. (2011). Effect of pumpkin root exudates on ex situ polychlorinated biphenyl (PCB) phytoextraction by pumpkin and weed species, *Environmental Science and Pollution Research*, 18, pp. 1536–1543.
- Helena, I.G., Celia, D.F. & Alexandra, B.R. (2013). Overview of in situ and ex situ remediation technologies for PCB-contaminated soils and sediments and obstacles for full-scale application, *Science of the Total Environment*, 445–446, pp. 237–260.
- Henriksson, S., Hagberg, J., Backstrom, M., Persson, I. & Lindstrom, G. (2013). Assessment of PCDD/Fs levels in soil at a contaminated sawmill site in Sweden – A GIS and PCA approach to interpret the contamination pattern and distribution, *Environmental Pollution*, 180, pp. 19–26.
- Kaliraj, S., Chandrasekar, N. & Magesh, N.S. (2013). Identification of potential groundwater recharge zones in Vaigai upper basin, Tamil Nadu, using GIS-based analytical hierarchical process (AHP) technique, *Arabian Journal of Geosciences*, 7, 4, pp. 1385–1401.
- Lee, C.S., Li, X.D., Shi, W.Z., Cheung, S.C. & Thornton, L. (2006). Metal contamination in urban, suburban, and country park soils of Hong Kong: A study based on GIS and multivariate statistics, *Science of the Total Environment*, 356, pp. 45–61.
- Lisowska, E. (2010). PAH soil concentrations in the vicinity of charcoal kilns in Bieszczady, *Archives of Environmental Protection*, 36, 4, pp. 41–54.
- Liu, X.M., Wu, J.J. & Xu, J.M. (2006). Characterizing the risk assessment of heavy metals and sampling uncertainty analysis in paddy field by geostatistics and GIS, *Environmental Pollution*, 141, 2, pp. 257–264.
- Patel, D.P., Dholakia, M.B., Naresh, N. & Srivastava, P.K. (2012). Water harvesting structure positioning by using geo-visualization concept and prioritization of mini-watersheds through morphometric analysis in the Lower Tapi Basin, *Journal of the Indian Chemical Society*, 40, 2, pp. 299–312.
- Ren, L.X., Lu, H.W., He, L. & Zhang, Y.M. (2014). Enhanced electrokinetic technologies with oxidization–reduction for organically-contaminated soil remediation, *Chemical Engineering Journal*, 247, pp. 111–124.
- Rosinska, A. & Dabrowska, L. (2011). PCBs and heavy metals in water and bottom sediments of the Kozłowa Góra Dam Reservoir, *Archives of Environmental Protection*, 37, 4, pp. 61–73.
- Sato, T., Todoroki, T., Shimoda, K., Terada, A. & Hosomi, M. (2010). Behavior of PCDDs/PCDFs in remediation of PCBs-contaminated sediments by ion, *Chemosphere*, 80, 2, pp. 184–189.
- van Es, B., Koren, B. & de Blank, H.J. (2014). Finite-difference schemes for anisotropic diffusion, *Journal of Computational Physics*, 272, pp. 526–549.
- Wlodarczyk-Makula, M. (2012). Half-life of carcinogenic Polycyclic Aromatic Hydrocarbons in stored sewage sludge, *Archives of Environmental Protection*, 38, 2, pp. 33–44.
- Wu, Y.H., Hung, M.C. & Patton, J. (2013). Assessment and visualization of spatial interpolation of soil pH values in farmland, *Precision Agriculture*, 14, 6, pp. 565–585.
- Yang, X.D., Cui, W.H., Wang, P. & Huang, Y.Q. (2007). The simulation of 3D structure of groundwater system based on Java/Java3D, *Geoinformatics*, 6753, pp. 75330–75330.
- Zhang, C.S., Luo, L., Xu, W.L. & Ledwith, V. (2008). Use of local Moran's I and GIS to identify pollution hotspots of Pb in urban soils of Galway, Ireland, *Science of The Total Environment*, 398, 1–3, pp. 212–221.